Unconventional tipping and winkled hysteresis loop in nonsmooth biophysical systems

Yoseb Kang,[1] Sangil Kim,[1] Ying-Cheng Lai,[2,3] and Younghae Do[4,*]

[1]*Department of Mathematics, Institute for Future Earth, Pusan National University, Busan, 46241, Republic of Korea*

[2]*School of Electrical, Computer and Energy Engineering, Arizona State University, Tempe, 85287, USA*

[3]*Department of Physics, Arizona State University, Tempe, 85287, USA*

[4]*Department of Mathematics, Nonlinear Dynamics & Mathematical Application Center, Kyungpook National University, Daegu, 41566, Republic of Korea*

(Dated: January 10, 2025)

A tipping point in nonlinear dynamical systems was previously understood as an abrupt transition from a high to a low stable steady state as a bifurcation parameter crosses a critical value. We uncover an unconventional tipping phenomenon in a class of non-autonomous nonsmooth biophysical systems, where the transition occurs through an intermediate, oscillatory state. Such a "stepping-stone" state also occurs in the reverse process of recovery, resulting in a "wrinkled" hysteresis loop. The dwelling time in the oscillatory state, e.g., the transient tipping time before the system settles in the low steady state, depends on the rate of the parameter change. The scaling laws of the transient tipping and recovery times are derived analytically. The intermediate state presents an opportunity for control intervention to prevent a healthy system from collapsing into a diseased state.

The broad phenomenon of tipping in dynamical systems has been understood as a sudden transition from one stable steady state to another as a bifurcation parameter changes through a critical point. Such systems are bistable and, as the parameter reverses its change, a transition to the original steady state can occur but at a parameter value differing from the tipping point, leading to a hysteresis loop that is quite common in bistable physical and biological systems [1–12]. A field in which tipping is of particular interest is ecosystems where the two stable states correspond to survival and extinction, respectively [13–38]. Global climate change makes tipping significantly more likely in critical natural systems such as the the Atlantic Meridional Overturning Circulation (AMOC) [39–41] that supports livable temperature conditions in Western Europe [42], where model-based statistical [43] and data-driven machine-learning [44] methods were recently developed to predict its potential tipping or collapse. Nonautonomous dynamical systems with some time-dependent bifurcation parameter are particularly vulnerable to tipping as it can be triggered by the time-rate change of the parameter, the phenomenon of rate-induced tipping [22, 45–50]. In most existing studies on tipping, the transition is typically abrupt through a saddle-node type of bifurcation.

In this Letter, we report a phenomenon in nonsmooth dynamical systems where tipping occurs in an unconventional manner that is characteristically different from any known scenario. In particular, the system still possesses two stable steady states. As a bifurcation parameter changes with time (thereby making the system nonautonomous), a transition from one stable steady state to another eventually occur, but through a "stepping-stone" type of intermediate attractor that is not a steady state but oscillatory. As illustrated in Fig. 1, at the first critical point, denoted as q_1, a transition from the high stable state to the intermediate attractor occurs, followed by a transition from this attractor to the low steady state at q_2. Likewise, in the reverse process of recovery, the system moves out of the low steady state to a different intermediate attractor at q_3, and the subsequent transition from this attractor to the high steady state at q_4 completes the hysteresis loop. While the two stable steady states do not depend on how fast the parameter changes, the intermediate attractor does depend on the time rate change of the parameter. To our knowledge, hysteresis loops in physical and biological systems reported in the literature are typically associated with abrupt but nonetheless smooth transitions between the two stable steady states [1–12], but in our case the loop becomes irregular and "winkled" due to the system's wandering on an oscillatory attractor before finally approaching a stable steady state. The dwelling or the transient time in the oscillatory state depends on the rate of parameter change and exhibits an algebraic scaling behavior, which can be understood analytically.

The prototypical model leading to the discovery of unconventional tipping and winkled hysteresis loop is the biophysical system underlying a quite common skin disease known as atopic dermatitis (AD) found in all age groups. AD is a prevalent dermatological condition with a complex etiology that spans genetic, immunological, and environmental factors [51–53]. This condition is known for its heterogeneous presentation across different age groups, ethnicities and genders, posing significant challenges to develop effective treatment [54–60]. The rarity of robust animal models further complicates the translation of theoretical research into clinical practice. Recently, the focus has shifted towards *in vivo*, *in vitro*, and *in silico* methods to dissect the pathophysiological underpinnings of AD and to identify critical therapeutic targets and biomarkers [61, 62], where nonlinear dynamical systems modeling and analysis become instrumental [63–67].

The biophysical mechanism of AD pathogenesis progression is captured by the model [64] in Fig. 1(a), as governed by the interactions between external pathogens and the skin barrier. Under normal conditions, small amounts of pathogens entering through compromised skin barriers are naturally contained and pose no significant threat. However, when the pathogen load exceeds a threshold, a critical point is reached,

* yhdo@knu.ac.kr

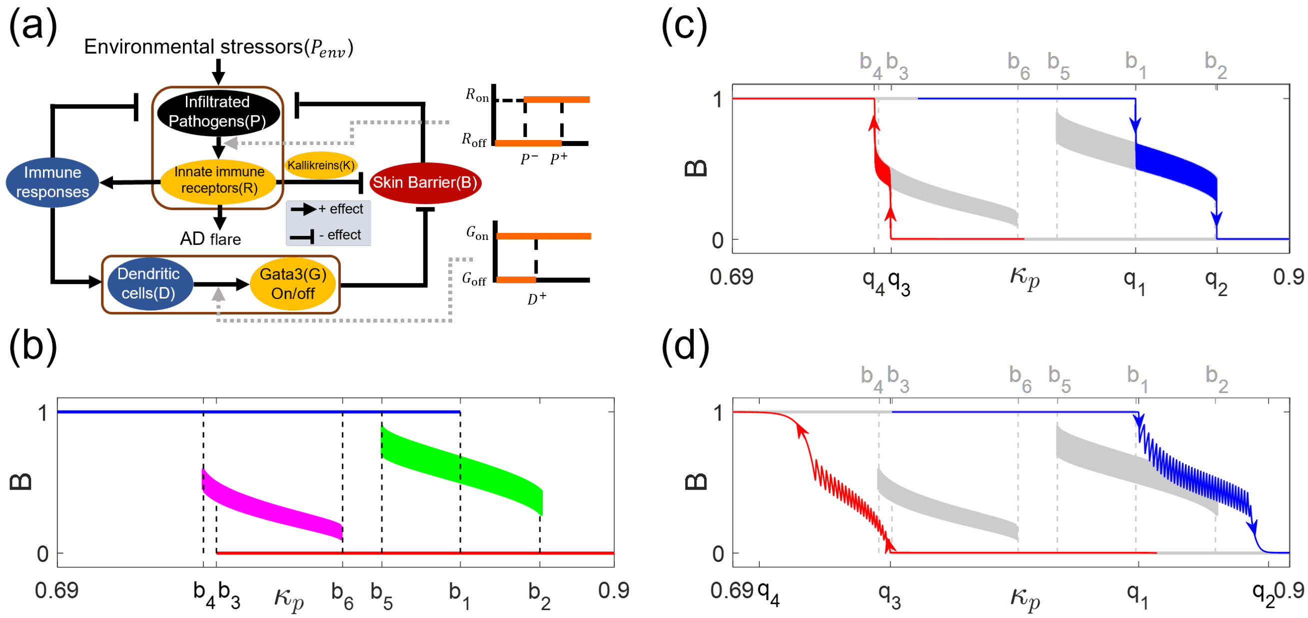

FIG. 1. AD system, unconventional tipping and wrinkled hysteresis loop. (a) The biophysical processes underlying AD leading to a nonsmooth dynamical system. (b) A bifurcation diagram with the nominal skin permeability κ_p, revealing multiple coexisting attractors. There are a low stable steady state $B = 0$ (red, denoted as C), a high stable steady state $B = 1$ (blue, H), and two oscillatory attractors in between (O_s - purple and O_m - green). The rate of pathogen eradication is fixed at $\alpha_I = 0.1$. There are six distinct bifurcation points b_i ($i = 1, \cdots, 6$). At each point, either a new attractor emerges or an existing attractor disappears. (c) For the corresponding nonautonomous system with $\kappa_p(t) = \kappa_p^s + \epsilon t$ ($\epsilon = 10^{-5}$), unconventional tipping occurs, where the system transits from H to O_m at $\kappa_p = q_1$, followed by another transition to C at q_2. The reverse process is also through two transitions: one at q_3 and another at q_4. The gray background marks the oscillatory attractors in (b). As a result of the four transitions, the hysteresis loop becomes wrinkled. (d) Similar transitions and wrinkled hysteresis loop for $\epsilon = 10^{-3}$.

at which physiological switches are activated, such as toll-like receptors (TLRs) and protease-activated receptor 2 (PAR2). As a result, an AD flare is triggered. The immune response includes the release of antimicrobial peptides that combat the invading pathogens and signal various immune mechanisms that mobilize dendritic cells to the lymph nodes. If the pathogen level decreases below a deactivation threshold, these switches are turned off, stopping the AD flare. Conversely, if the dendritic cell count in the lymph nodes surpasses a second critical threshold, a further, irreversible change in the immune state occurs, exacerbating the skin condition. Because of the activation and deactivation of the switches, the underlying dynamical system is nonsmooth:

$$\begin{aligned}
\frac{dP}{dt} &= \frac{P_{\text{env}}\kappa_p}{1+\gamma_B B(t)} - \alpha_I R(t)P(t) - \delta_p P(t), \\
\frac{dB}{dt} &= \frac{\kappa_B[1-B(t)]}{[1+\gamma_R R(t)][1+\gamma_G G(t)]} - \delta_B K(t)B(t), \qquad (1)\\
\frac{dD}{dt} &= \kappa_D R(t) - \delta_D D(t),
\end{aligned}$$

where $P(t) \geq 0$, $0 \leq B(t) \leq 1$ and $D(t) \geq 0$ denote the infiltrated pathogen load (in milligrams per milliliter), the strength of barrier integrity (relative to the maximum strength), and the concentration of dendritic cells (DCs) in the lymph node (cells per milliliter), respectively. The typical parameter values are listed in Tab. S1 in Supplementary Information (SI) [68].

The structure of the skin barrier is dependent on the proteins keratin and filaggrin (FLG), and the extracellular matrix containing lipids, structural proteins, and the serine protease subgroup kallikreins. Dysfunction of these components can result in barrier defects, as typically found in loss-of-function mutations of the FLG gene [69]. The AD model (1) utilizes switches to describe the activation of the immune system, as shown in Fig. 1(a). In particular, the switches $R(t)$, $G(t)$ and $K(t)$ depict the levels of activated immune receptors, *Gata*3 transcription relative to the maximum transcription level, and active kallikreins, respectively, which are given by $R(t) = R_{\text{off}}$ for $P(t) < P^-$ or $P^- \leq P(t) \leq P^+$ and $R(t^-) = R_{\text{off}}$; $R(t) = R_{\text{on}}$ for $P(t) > P^+$ or $P^- \leq P(t) \leq P^+$ and $R(t^-) = R_{\text{on}}$}; $K(t) = K_{\text{off}}$ for $P(t) < P^-$ or $P^- \leq P(t) \leq P^+$ and $R(t^-) = R_{\text{off}}$; $K(t) = m_{\text{on}}P(t) - \beta$ for $P(t) > P^+$ or $P^- \leq P(t) \leq P^+$ and $R(t^-) = R_{\text{on}}$; $G(t) = G_{\text{off}}$ for $D(t) < D^+$ and $G(t^-) = G_{\text{off}}$; $G(t) = G_{\text{on}}$ for $D(t) \geq D^+$ or $G(t^-) = G_{\text{on}}$, where R_{on}, R_{off}, G_{on}, G_{off} and K_{off} are parameters characterizing the activating or inactivating constant-level of the switches, but K_{on} depends on $P(t)$: $K_{\text{on}} = m_{\text{on}}P(t) - \beta$, and the two switches R and K work together simultaneously.

The AD system (1) exhibits complicated dynamical phenomena including multistability, transients and nonsmooth bifurcations [66, 67]. Previous works [64, 66] revealed four distinct attractors corresponding to the four stages of AD: healthy recovery (H), chronic damage (C), mild oscillations (O_m), and severe oscillations (O_s). Two key parameters are the nominal skin permeability κ_p and the rate α_I of pathogen eradication. Figure 1(b) shows a typical bifurcation diagram with κ_p for $\alpha_I = 0.1$, where there are six distinct bifurcation points b_i ($i = 1, \ldots, 6$) with four attractors in different parameter intervals. In particular, for $\kappa_p < b_4$, the high steady state is the only attractor. As κ_p increases through b_4, the attractor O_s emerges. For $b_4 \leq \kappa_p \leq b_3$, the system has two coexisting attractors. At $\kappa_p = b_3$, a low steady state attractor is born. For $b_3 \leq \kappa_p \leq b_6$, the system has three coexisting attractors. At b_6, O_s is destroyed and the system has two coexisting steady-state attractors for $b_6 \leq \kappa_p \leq b_5$. At b_5, the mild oscillatory attractor O_m is created and the system has three coexisting attractors again for $b_5 \leq \kappa_p \leq b_1$. At b_1 and b_2, respectively, the high steady state and mild oscillatory attractors disappear, and the system has two coexisting attractors for $b_1 \leq \kappa_p \leq b_2$. For $\kappa_p > b_2$, the low steady state is the only attractor.

Clinically, the bifurcation diagram in Fig. 1(b) vividly captures the process of disease progression in AD patients. Note that κ_p characterizes the skin condition, where large values of κ_p correspond to a more deteriorated condition. For $\kappa_p < b_4$, patient's skin condition is healthy, where the high steady state is the only attractor in the system. As κ_p increases through b_4, clinic symptoms of varying degrees as characterized by the occurrence of the oscillatory attractors and the low steady state. For $\kappa_p > b_2$, AD has evolved into the most severe stage.

The AD system (1) is nonautonomous as the skin condition changes with time for a variety of reasons including aging. To model this feature, we set the nominal skin permeability as a function of time [70, 71]: $\kappa_p(t) = \kappa_p^s \pm \epsilon t$, where κ_p^s is the initial value and ϵ is the linear ramping rate. The forward ($+$) and backward ($-$) conditions indicate that the skin condition will deteriorate and improve with time, respectively. Figure 1(c) shows, for $\epsilon = 10^{-5}$ and $\kappa_p^s = 0.76$ (0.8), forward (backward) trajectories. As the skin conditions deteriorate, a tipping transition occurs in the relative strength $B(t)$ of the barrier integrity at q_1 from the high steady state to the oscillatory state O_m (the blue trajectory, corresponding to mild skin disease). The system remains in O_m until κ_p reaches the second critical point $q_2 > q_1$, at which $B(t)$ drops to near zero, signifying reaching the most severe stage of AD. For reference, the bifurcation diagram in Fig. 1(b) for the autonomous system is included in Fig. 1(c) as the gray background. In the nonautonomous system, both transitions at q_1 and q_2 are abrupt, which is characteristic of tipping. Overall, the tipping from the high healthy state to the intermediate oscillatory state, the system's maintaining in this state for a finite parameter interval (equivalently, a finite amount of time) and the second tipping to the low steady state, constitute an unconventional, two-stage tipping transition. This makes the tipping branch of the hysteresis loop rippled, in contrast to the tipping behavior directly from the high to the low stable steady state in smooth dynamical systems [1–12].

A similar phenomenon occurs in the backward direction of the parameter variation: $\kappa_p(t) = \kappa_p^s - \epsilon t$, where the skin condition is improved. At the transition point $q_3 < q_1$, a sudden transition from the low steady state to another intermediate oscillatory state, O_s, occurs. The system stays in O_s for a finite parameter interval (time) before an abrupt transition back to the high stable steady state at $q_4 < q_3$. Owing to the dwelling in the oscillatory state O_s, the recovery process from the low to the high steady state is also unconventional, contributing to an irregular branch of the hysteresis loop. Compared with a typical hysteresis loop in smooth dynamical systems [1–12], the overall hysteresis loop in Fig. 1(c) is "wrinkled."

Two remarks are in order. First, in the nonautonomous AD system, the tipping points q_i are different from the corresponding bifurcating points b_i in the autonomous system, as indicated in Fig. 1(c). This difference can be understood analytically (SI [68]). Second, the phenomena of unconventional tipping and wrinkled hysteresis loop can occur for different time rate change of the bifurcation parameter, as exemplified in Fig. 1(d) for $\epsilon = 10^{-3}$, a rate that is two orders of magnitude higher than that in Fig. 1(c). At this rate, the first tipping occurs at approximately the same point q_1 but the oscillatory state of mild AD lasts in a larger parameter interval as a higher critical value q_2 is required for the system to switch to the low steady state associated with severe AD. Likewise, while the first recovery point q_3 in Figs. 1(c) and 1(d) are approximately the same, the oscillatory state lasts through a larger parameter interval and the skin condition as characterized by the value of κ_p needs to be significantly more improved for a full recovery at $\epsilon = 10^{-3}$ than at $\epsilon = 10^{-5}$. In fact, the quantities $q_i - b_i$ ($i = 1, 2, 3, 4$), the differences between the transition points in the nonautonomous system and their corresponding bifurcation points in the autonomous system, depend on the rate ϵ and obey scaling laws. In spite of the differences in the detailed transitions, the tipping and recovery transitions contain multiple stages through some oscillatory state as the "springboard" and the overall hysteresis loop remains wrinkled.

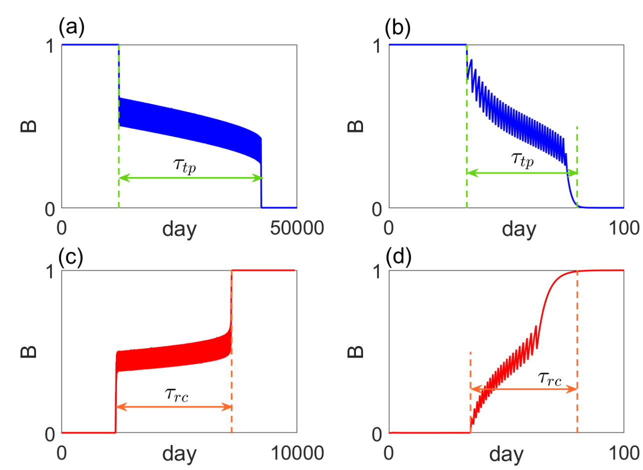

FIG. 2. Transient tipping and recovery process. (a,b) A relatively long and short transient process for the tipping from the high to low stable state to finish for $\epsilon = 10^{-5}$ and 10^{-3}. respectively. (c,d) Similar transient recovery process for $\epsilon = 10^{-5}$ and 10^{-3}, respectively. For the two values of the ramping rate, the difference in the transient time is more than the time difference as determined by the rate.

The unconventional, two-stage tipping process in the AD system, as demonstrated in Figs. 1(c) and 1(d), is drastically different from conventional tipping in smooth dynamical systems. To better appreciate the difference, we note that, in a nonautonomous smooth system, the tipping occurs almost instantaneously: due to the little parameter change required at the critical point for tipping, practically it takes an infinitesimal amount time for the transition from the high to the low stable steady state to occur. However, in the nonsmooth AD system, the time for tipping, or the transient tipping time between the two consecutive tipping points denoted as $\tau_{\rm tp}$, to occur can be quite long. Figures 2(a) and 2(b) show, for $\epsilon = 10^{-5}$ and 10^{-3}, respectively, the length of the transient tipping time, where the difference in the transient time in the two cases is about three orders of magnitude (approximately 10 times larger than the difference in the parameter ramping rate). Similarly, the recovery process also involves a long transient process, as illustrated in Figs. 2(c) and 2(d).

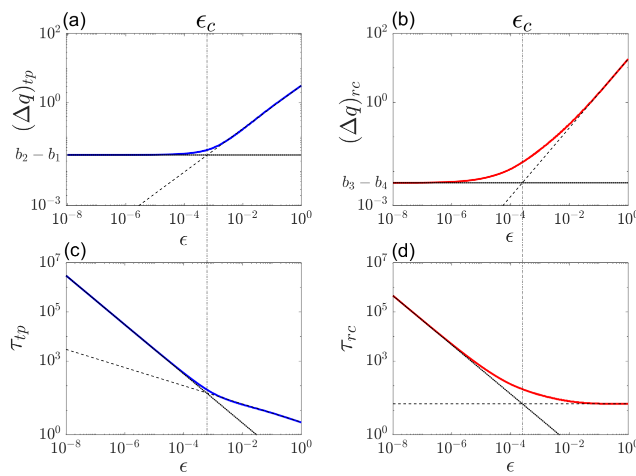

FIG. 3. Scaling of tipping and recovery parameter intervals, and of the transient tipping and recovery times with the parameter ramping rate. (a,b) Scaling of $(\Delta q)_{\rm tp}(\epsilon)$ and $(\Delta q)_{\rm rc}(\epsilon)$, respectively. The two horizontal asymptotic dotted lines correspond to the difference between the two consecutive bifurcation points, i.e., $b_2 - b_1$ and $b_3 - b_4$, respectively. (c,d) Scaling of $\tau_{\rm tp}(\epsilon)$ and $\tau_{\rm rc}(\epsilon)$, respectively.

To characterize unconventional tipping and the wrinkled hysteresis loop, we examine four quantities: (1) the tipping parameter interval $(\Delta q)_{\rm tp} \equiv q_2 - q_1$ [cf., Figs. 1(c,d)] (2) the recovery parameter interval $(\Delta q)_{\rm rc} \equiv q_3 - q_4$ [cf., Figs. 1(c,d)], (3) the transient tipping time $\tau_{\rm tp}$ [cf., Figs. 2(a,b)] and (4) the transient recovery time $\tau_{\rm rc}$ [cf., Figs. 2(c,d)]. As these quantities depend on the parameter ramping rate ϵ, we ask what scaling relations between them and ϵ are. Figures 3(a) and 3(b) show the numerically obtained representative scaling behavior of $(\Delta q)_{\rm tp}(\epsilon)$ and $(\Delta q)_{\rm rc}(\epsilon)$, respectively. For a slow rate $\epsilon \ll \epsilon_c$, $(\Delta q)_{\rm tp}(\epsilon)$ and $(\Delta q)_{\rm rc}(\epsilon)$ approach the parameter difference between the two static bifurcation points, $b_2 - b_1$ and $b_3 - b_4$, respectively. However, for $\epsilon \gg \epsilon_c$, $(\Delta q)_{\rm tp}(\epsilon)$ and $(\Delta q)_{\rm rc}(\epsilon)$ increase algebraically with ϵ, with the respective scaling exponent $\beta_{\rm tp} \approx 0.63$ and $\beta_{\rm rc} \approx 1$. We have

$$(\Delta q)_{\rm tp}(\epsilon) \sim \begin{cases} \epsilon^{\beta_{\rm tp}} & \epsilon > \epsilon_c, \\ b_2 - b_1 & \epsilon < \epsilon_c, \end{cases} \tag{2}$$

$$(\Delta q)_{\rm rc}(\epsilon) \sim \begin{cases} \epsilon^{\beta_{\rm rc}} & \epsilon > \epsilon_c, \\ b_3 - b_4 & \epsilon < \epsilon_c. \end{cases} \tag{3}$$

These scaling results indicate that, for a more rapid change of the parameter, both the tipping and recovery processes require a larger parameter change to complete. The scaling relations (2) and (3) can be derived analytically (SI [68]).

The relations $\tau_{\rm tp}(\epsilon) = (\Delta q)_{\rm tp}(\epsilon)/\epsilon$ and $\tau_{\rm rc}(\epsilon) = (\Delta q)_{\rm rc}(\epsilon)/\epsilon$ lead to the following algebraic scaling of the transient tipping and recovery times:

$$\tau_{\rm tp}(\epsilon) \sim \begin{cases} \epsilon^{\beta_{\rm tp}-1}, & \epsilon > \epsilon_c, \\ \epsilon^{-1}, & \epsilon < \epsilon_c, \end{cases} \tag{4}$$

$$\tau_{\rm rc}(\epsilon) \sim \begin{cases} \text{constant}, & \epsilon > \epsilon_c, \\ \epsilon^{-1}, & \epsilon < \epsilon_c, \end{cases} \tag{5}$$

as exemplified in Figs. 3(c) and 3(d), respectively. Note that, for $\epsilon \gg \epsilon_c$, the transient recovery time $\tau_{\rm rc}(\epsilon)$ approaches a constant.

To summarize, we have uncovered a type of tipping behavior in a class nonautonomous nonsmooth biophysical systems that is quite distinct from the conventional tipping so far reported in the literature. Such a system describes the evolution of common skin diseases with different clinically distinguishable stages. The main feature of the unconventional tipping is that the transition from a high to a low stable steady state occurs through an intermediate oscillatory state in an extended duration of parameter changes or time. A similar scenario arises during the recovery process from the low to the high steady state. As a result, tipping and recovery are no longer "instantaneous" but transient, and the hysteresis loop exhibits a wrinkled structure. The clinical significance of these phenomena are the following. Given that transition from the high steady state to the intermediate oscillatory state corresponds to a sudden deterioration of the skin barrier with alternating symptoms and a further transition to the low state marks the onset of severe skin disease, the emergence of the intermediate state presents an opportunity for control intervention to prevent a healthy system from collapsing completely into the diseased state. Nonsmooth dynamics arise in biological and physical systems. Our findings indicate that tipping and hysteresis loop can manifest themselves in ways that have not been previously recognized.

This work was supported by the National Research Foundation of Korea through Grants Nos. NRF-2022R1A5A1033624, NRF-2022R1A2C3011711, and by Global-Learning & Academic research institution for Master's·PhD students, and Postdocs (LAMP) Program of the National Research Foundation of Korea grant funded by the Ministry of Education (No. RS-2023-00301938). The work at Arizona State University was supported by AFOSR through Grant No. FA9550-21-1-0438.

[1] D. Angeli, J. Ferrell, and E. D. Sontag, Detection of multistability, bifurcations, and hysteresis in a large class of biological positive-feedback systems, Proc. Nat. Acad. Sci. (USA) **101**, 1822 (2004).

[2] D. M. Umulis, M. Serpe, M. B. O. O'Connor, and H. G. Othmer, Robust, bistable patterning of the dorsal surface of the drosophila embryo, Proc. Nat. Acad. Sci. (USA) **103**, 11613 (2006).

[3] C. Argyropoulos, P.-Y. Chen, F. Monticone, G. D'Aguanno, and A. Alù, Nonlinear plasmonic cloaks to realize giant all-optical scattering switching, Phys. Rev. Lett. **108**, 263905 (2012).

[4] J. Sheng, U. Khadka, and M. Xiao, Realization of all-optical multistate switching in an atomic coherent medium, Phys. Rev. Lett. **109**, 223906 (2012).

[5] M. Wu, R.-Q. Su, X.-H. Li, T. Ellis, Y.-C. Lai, and X. Wang, Engineering of regulated stochastic cell fate determination, Proc. Nat. Acad. Sci. (USA) **110**, 10610 (2013).

[6] C. K. Andersen and K. Mølmer, Circuit qed flip-flop memory with all-microwave switching, Phys. Rev. Appl. **3**, 024002 (2015).

[7] L.-Z. Wang, R.-Q. Su, Z.-G. Huang, X. Wang, W.-X. Wang, C. Grebogi, and Y.-C. Lai, A geometrical approach to control and controllability of nonlinear dynamical networks, Nat. Commun. **7**, 11323 (2016).

[8] F.-Q. Wu, R.-Q. Su, Y.-C. Lai, and X. Wang, Engineering of a synthetic quadrastable gene network to approach waddington landscape and cell fate determination, eLife **6**, e23702 (2017).

[9] V. Bacot, S. Perrard, M. Labousse, Y. Couder, and E. Fort, Multistable free states of an active particle from a coherent memory dynamics, Phys. Rev. Lett. **122**, 104303 (2019).

[10] D. Winters, M. A. Abeed, S. Sahoo, A. Barman, and S. Bandyopadhyay, Reliability of magnetoelastic switching of nonideal nanomagnets with defects: A case study for the viability of straintronic logic and memory, Phys. Rev. Appl. **12**, 034010 (2019).

[11] R. Fermin, N. M. A. Scheinowitz, J. Aarts, and K. Lahabi, Mesoscopic superconducting memory based on bistable magnetic textures, Phys. Rev. Res. **4**, 033136 (2022).

[12] M.-X. Bi, H. Fan, X.-H. Yan, and Y.-C. Lai, Folding state within a hysteresis loop: Hidden multistability in nonlinear physical systems, Phys. Rev. Lett. **132**, 137201 (2024).

[13] M. Scheffer, *Ecology of Shallow Lakes* (Springer, 2004).

[14] M. Scheffer, J. Bascompte, W. A. Brock, V. Brovkin, S. R. Carpenter, V. Dakos, H. Held, E. H. Van Nes, M. Rietkerk, and G. Sugihara, Early-warning signals for critical transitions, Nature **461**, 53 (2009).

[15] M. Scheffer, Complex systems: foreseeing tipping points, Nature **467**, 411 (2010).

[16] D. B. Wysham and A. Hastings, Regime shifts in ecological systems can occur with no warning, Ecol. Lett. **13**, 464 (2010).

[17] J. M. Drake and B. D. Griffen, Early warning signals of extinction in deteriorating environments, Nature **467**, 456 (2010).

[18] J. M. T. Thompson and J. Sieber, Predicting climate tipping as a noisy bifurcation: a review, Int. J. Bif. Chaos **21**, 399 (2011).

[19] L. Chen, R. Liu, Z.-P. Liu, *et al.*, Detecting early-warning signals for sudden deterioration of complex diseases by dynamical network biomarkers, Sci. Rep. **2**, 342 (2012).

[20] C. Boettiger and A. Hastings, Quantifying limits to detection of early warning for critical transitions, J. R. Soc. Interface **9**, 2527 (2012).

[21] L. Dai, D. Vorselen, K. S. Korolev, and J. Gore, Generic indicators for loss of resilience before a tipping point leading to population collapse, Science **336**, 1175 (2012).

[22] P. Ashwin, S. Wieczorek, R. Vitolo, and P. Cox, Tipping points in open systems: bifurcation, noise-induced and rate-dependent examples in the climate system, Phil. Trans. R. Soc. A **370**, 1166 (2012).

[23] T. M. Lenton, V. N. Livina, V. Dakos, E. H. van Nes, and M. Scheffer, Early warning of climate tipping points from critical slowing down: comparing methods to improve robustness, Phil. Trans. R. Soc. A **370**, 1185 (2012).

[24] A. D. Barnosky, E. A. Hadly, J. Bascompte, E. L. B. J. H. Brown, M. Fortelius, W. M. Getz, J. Harte, A. Hastings, P. A. Marquet, N. D. Martinez, A. Mooers, P. Roopnarine, G. Vermeij, J. W. Williams, R. Gillespie, J. Kitzes, C. Marshall, N. Matzke, D. P. Mindell, E. Revilla, and A. B. Smith, Approaching a state shift in earth's biosphere, Nature **486**, 52 (2012).

[25] C. Boettiger and A. Hastings, Tipping points: From patterns to predictions, Nature **493**, 157 (2013).

[26] J. M. Tylianakis and C. Coux, Tipping points in ecological networks, Trends Plant Sci. **19**, 281 (2014).

[27] J. J. Lever, E. H. Nes, M. Scheffer, and J. Bascompte, The sudden collapse of pollinator communities, Ecol. Lett. **17**, 350 (2014).

[28] T. S. Lontzek, Y.-Y. Cai, K. L. Judd, and T. M. Lenton, Stochastic integrated assessment of climate tipping points indicates the need for strict climate policy, Nat. Clim. Change **5**, 441 (2015).

[29] S. Gualdia, M. Tarziaa, F. Zamponic, and J.-P. Bouchaudd, Tipping points in macroeconomic agent-based models, J. Econ. Dyn. Control **50**, 29 (2015).

[30] J. Jiang, Z.-G. Huang, T. P. Seager, W. Lin, C. Grebogi, A. Hastings, and Y.-C. Lai, Predicting tipping points in mutualistic networks through dimension reduction, Proc. Nat. Acad. Sci. (USA) **115**, E639 (2018).

[31] B. Yang, M. Li, W. Tang, S. Liu, Weixinand Zhang, L. Chen, and J. Xia, Dynamic network biomarker indicates pulmonary metastasis at the tipping point of hepatocellular carcinoma, Nat. Commun. **9**, 678 (2018).

[32] J. Jiang, A. Hastings, and Y.-C. Lai, Harnessing tipping points in complex ecological networks, J. R. Soc. Interface **16**, 20190345 (2019).

[33] M. Scheffer, *Critical Transitions in Nature and Society*, Vol. 16 (Princeton Univ. Press, 2020).

[34] Y. Meng, J. Jiang, C. Grebogi, and Y.-C. Lai, Noise-enabled species recovery in the aftermath of a tipping point, Phys. Rev. E **101**, 012206 (2020).

[35] Y. Meng, Y.-C. Lai, and C. Grebogi, Tipping point and noise-induced transients in ecological networks, J. R. Soc. Interface **17**, 20200645 (2020).

[36] P. E. O'Keeffe and S. Wieczorek, Tipping phenomena and points of no return in ecosystems: Beyond classical bifurcations, SIAM J. Appl. Dyn. Syst. **19**, 2371 (2020).

[37] Y. Meng and C. Grebogi, Control of tipping points in stochastic mutualistic complex networks, Chaos **31**, 023118 (2021).

[38] Y. Meng, Y.-C. Lai, and C. Grebogi, The fundamental benefits of multiplexity in ecological networks, J. R. Soc. Interface **19**, 20220438 (2022).

[39] M. W. Buckley and J. Marshall, Observations, inferences, and mechanisms of the Atlantic Meridional Overturning Circulation: A review, Rev. Geophys. **54**, 5 (2016).

[40] J. Lohmann and P. D. Ditlevsen, Risk of tipping the overturning

circulation due to increasing rates of ice melt, Proc. Natl. Acad. Sci. (USA) **118**, e2017989118 (2021).

[41] L. C. Jackson, A. Biastoch, M. W. Buckley, D. G. Desbruyères, E. Frajka-Williams, B. Moat, and J. Robson, The evolution of the North Atlantic Meridional overturning Circulation since 1980, Nat. Rev. Earth Environ. **3**, 241 (2022).

[42] K. E. Trenberth, Y. Zhang, J. T. Fasullo, and L. Cheng, Observation-based estimates of global and basin ocean meridional heat transport time series, J. Clim. **32**, 4567 (2019).

[43] P. Ditlevsen and S. Ditlevsen, Warning of a forthcoming collapse of the Atlantic Meridional Overturning Circulation, Nat. Commun **14**, 4254 (2023).

[44] S. Panahi, L.-W. Kong, M. Moradi, Z.-M. Zhai, B. Glaz, M. Haile, and Y.-C. Lai, Machine learning prediction of tipping in complex dynamical systems, Phys. Rev. Res. **6**, 043194 (2024).

[45] P. Ashwin, C. Perryman, and S. Wieczorek, Parameter shifts for nonautonomous systems in low dimension: bifurcation-and rate-induced tipping, Nonlinearity **30**, 2185 (2017).

[46] A. Vanselow, S. Wieczorek, and U. Feudel, When very slow is too fast-collapse of a predator-prey system, J. Theo. Biol. **479**, 64 (2019).

[47] A. D. Synodinos, R. Karnatak, C. A. Aguilar-Trigueros, P. Gras, T. Heger, D. Ionescu, S. Maaß, C. L. Musseau, G. Onandia, A. Planillo, *et al.*, The rate of environmental change as an important driver across scales in ecology, Oikos , e09616 (2022).

[48] S. Panahi, Y. Do, A. Hastings, and Y.-C. Lai, Rate-induced tipping in complex high-dimensional ecological networks, Proc. Nat. Acad. Sci. (USA) **120**, e2308820120 (2023).

[49] U. Feudel, Rate-induced tipping in ecosystems and climate: the role of unstable states, basin boundaries and transient dynamics, Nonlinear Proc. Geophys. **30**, 481 (2023).

[50] A. Vanselow, L. Halekotte, P. Pal, S. Wieczorek, and U. Feudel, Rate-induced tipping can trigger plankton blooms, Theo. Ecol. **17**, 89 (2024).

[51] D. Y. Leung, Pathogenesis of atopic dermatitis, J. Allergy Clin. Immunol. **104**, S99 (1999).

[52] M. Furue, S. Yamazaki, K. Jimbow, T. Tsuchida, M. Amagai, T. Tanaka, K. Matsunaga, M. Muto, E. Morita, M. Akiyama, Y. Soma, T. Terui, and M. Manabe, Prevalence of dermatological disorders in japan: a nationwide, cross-sectional, seasonal, multicenter, hospital-based study, J. Dermatol. **38**, 310 (2011).

[53] K. Abuabara, D. J. Margolis, and S. M. Langan, The long-term course of atopic dermatitis, Dermatol. Clin. **35**, 291 (2017).

[54] S. Illi, E. von Mutius, S. Lau, R. Nickel, C. Grüber, B. Niggemann, U. Wahn, and M. A. S. G. et al., The natural course of atopic dermatitis from birth to age 7 years and the association with asthma, J. Allergy Clin. Immunol. **113**, 925 (2004).

[55] D. Garmhausen, T. Hagemann, T. Bieber, I. Dimitriou, R. Fimmers, T. Diepgen, and N. Novak, Characterization of different courses of atopic dermatitis in adolescent and adult patients, Allergy **68**, 498 (2013).

[56] T. Bieber, M. Angelo, C. A. Akdis, C. Traidl-Hoffmann, R. Lauener, G. Schäppi, and P. Schmid-Grendelmeier, Clinical phenotypes and endophenotypes of atopic dermatitis: where are we, and where should we go?, J. Allergy Clin. Immunol. **139**, S58 (2017).

[57] C. Roduit, R. Frei, M. Depner, A. M. Karvonen, H. Renz, C. Braun-Fahrländer, E. Schmausser-Hechfellner, J. Pekkanen, J. Riedler, and J. e. a. Dalphin, Phenotypes of atopic dermatitis depending on the timing of onset and progression in childhood, JAMA Pediatr. **171**, 655 (2017).

[58] Y. W. Yew, J. P. Thyssen, and J. I. Silverberg, A systematic review and meta-analysis of the regional and age-related differences in atopic dermatitis clinical characteristics, J. Am. Acad. Dermatol. **80**, 390 (2019).

[59] Y. J. Kim, S. J. Yun, J.-B. Lee, S. J. Kim, Y. H. Won, and S.-C. Lee, Four years prospective study of natural history of atopic dermatitis aged 7˜ 8 years at an individual level: a community-based survey by dermatologists' skin examination in childhood, Ann. Dermatol. **28**, 684 (2016).

[60] D. Y. Leung, Atopic dermatitis: new insights and opportunities for therapeutic intervention, J. Allergy Clin. Immunol. **105**, 860 (2000).

[61] P. Christodoulides, Y. Hirata, E. Domínguez-Hüttinger, S. G. Danby, M. J. Cork, H. C. Williams, K. Aihara, and R. J. Tanaka, Computational design of treatment strategies for proactive therapy on atopic dermatitis using optimal control theory, Philos. Trans. R. Soc. A **375**, 20160285 (2017).

[62] K. Eyerich, S. J. Brown, B. E. P. White, R. J. Tanaka, R. Bissonette, S. Dhar, T. Bieber, D. J. Hijnen, E. Guttman-Yassky, and A. e. a. Irvine, Human and computational models of atopic dermatitis: A review and perspectives by an expert panel of the international eczema council, J. Allergy Clin. Immunol. **143**, 36 (2019).

[63] R. J. Tanaka and M. Ono, Skin disease modeling from a mathematical perspective, J.Invest. Dermatol. **133**, 1472 (2013).

[64] E. Domínguez-Hüttinger, P. Christodoulides, K. Miyauchi, A. D. Irvine, M. Okada-Hatakeyama, M. Kubo, and R. J. Tanaka, Mathematical modeling of atopic dermatitis reveals "double-switch" mechanisms underlying 4 common disease phenotypes, J. Allergy Clin. Immunol. **139**, 1861 (2017).

[65] G. Tanaka, E. Domínguez-Hüttinger, P. Christodoulides, K. Aihara, and R. J. Tanaka, Bifurcation analysis of a mathematical model of atopic dermatitis to determine patient-specific effects of treatments on dynamic phenotypes, J. Theor. Biol. **448**, 66 (2018).

[66] Y. Kang, E. H. Lee, S. Kim, Y. H. Jang, and Y. Do, Complexity and multistability of a nonsmooth atopic dermatitis system, Chaos, Solitons & Fractals **153**, 111575 (2021).

[67] Y. Kang, J. Hwang, Y.-C. Lai, H. Choi, and Y. Do, A nonlinear transient-dynamics approach to atopic dermatitis: Role of spontaneous remission, Chaos, Solitons & Fractals **179**, 114464 (2024).

[68] Supplementary Information provides details elaborating the results in the main text. It is helpful but not essential for understanding the main results of the paper. It contains mainly the analytic derivations of the scaling results.

[69] D. Bending and M. Ono, Interplay between the skin barrier and immune cells in patients with atopic dermatitis unraveled by means of mathematical modeling, J. Allergy Clin. Immunol. **139**, 1790 (2017).

[70] Y.-H. Liao, S.-Y. Chen, S.-Y. Chou, P.-H. Wang, M.-R. Tsai, and C.-K. Sun, Determination of chronological aging parameters in epidermal keratinocytes by in vivo harmonic generation microscopy, Biomed. Opt. Express **4**, 77 (2013).

[71] C. E. Rübe, C. Bäumert, N. Schuler, A. Isermann, Z. Schmal, M. Glanemann, C. Mann, and H. Scherthan, Human skin aging is associated with increased expression of the histone variant h2a. j in the epidermis, NPJ Aging. Mech. Dis. **7**, 7 (2021).